IORT	Intraoperative radiotherapy
LCIS	Lobular carcinoma in situ
LVSI	Lymph-vascular space invasion
PBI	Partial breast irradiation
PMMA	Polymethyl methacrylate
RT	Radiotherapy
SN Bx	Sentinel lymph node biopsy
TARGIT	Targeted intraoperative radiotherapy
WBI	Whole breast external irradiation therapy

Introduction

There is no difference in disease-free or overall survival rates between mastectomy or lumpectomy with whole breast external irradiation therapy (WBI) for women with early breast cancer [1, 2]. Thus, the standard treatment for early breast cancer is breast-conserving therapy (BCT) with WBI, and local control plays a crucial role in survival [3, 4]. On the other hand, the main objective of radiotherapy after BCT is also considered to be the destruction of residual cancer cells in the operative field, and partial breast irradiation (PBI) has been tested in clinical trials for selected patients. Adequate local control, minimal toxicity, and good cosmetic appearance were reported in these selected patients [5]. Intraoperative radiotherapy (IORT) is one of these PBI methods which have been recently used in early-stage breast cancer, but being outside the setting of a clinical trial, it has not yet been recommended [5, 6]. To date, IORT remains investigational until information on its long-term efficacy and safety becomes available. IORT has been used mainly at the European Institute of Oncology (EIO) in Italy since 1999 [7–11]. Prospective trials to investigate the tolerance to increased IORT doses are required. The ultimate aim is to introduce the use of 21 Gy in the context of BCT, which is biologically equivalent to a full dose of conventional WBI [7–10]. Although no data are available for tolerance to doses of IORT in Asian breast cancer patients, a recent Japanese phase I/II study was published [12, 13]. The dose of 21 Gy was feasible, as well as in European breast cancer patients. However, in the previous report [13], the MOBETRON® device was used in the operating room, which did not require the patient to be transported elsewhere during the surgical procedure. Feasibility cannot be determined if the device is not in the operating room because the patient needs to be transported to the radiation therapy room under general anesthesia.

The purpose of this prospective single-center pilot study was to test the feasibility of IORT at a single dose of 21 Gy in an institution which requires transport of the patient under general anesthesia. This paper mainly reports the results of feasibility, and the merits and limitations of IORT for early breast cancer are discussed.

Patients and methods

Study design

This was a single arm non-randomized pilot study, which was approved by the research ethics review committee. The primary endpoint was early toxicity (within 3 months). The secondary endpoint was late toxicity. This study was performed in accordance with the Declaration of Helsinki and Good Clinical Practice. Written informed consent was obtained from all patients prior to the study.

Eligibility criteria

Patients with histologically or cytologically proven primary early breast cancer were eligible. Inclusion criteria were as follows: (1) clinical tumor size (US and CT or MRI) less than 2.5 cm; (2) patient's desire for BCS; (3) age older than 50 years; (4) surgical margin more than 1 cm; (5) intraoperative pathologically free margins; and (6) sentinel node negative. Exclusion criteria were (1) contraindications to radiation therapy; (2) past radiation therapy for the same breast or chest; (3) extensive intraductal component; and (4) a tumor located in the axillary tail of the breast.

Study assessments

Early toxicity was evaluated by the National Cancer Institute Common Terminology Criteria for Adverse Events (NCI CTCAE), version 4.0 (Table 1). Several breast surgeons and radiation oncologists independently assessed these toxicities. After surgery, each patient was scheduled for weekly evaluations during the first month, then at intervals of 3 months during the first year, and every 6 months thereafter for 5 years with physical examinations and photographic records.

Procedures

The operative procedures performed were as follows: (1) Sentinel lymph node biopsy. (2) Partial resection with at least a 1-cm margin around the tumor. (3) Microscopic assessment of margins by frozen sections. (4) Placement of a dual-layer plate comprising acrylic resin and copper [14] between the gland and the pectoralis muscle to protect the thoracic wall. The disk was larger than the breast target size, and the disks were prepared with diameters of 6–10 cm at 1-cm intervals. The gland was sutured

Table 1 Definitions of the toxicities (NCI CTCAE v4.0)

Adverse event	Grade 1	Grade 2	Grade 3	Grade 4	Grade 5
Fibrosis deep connective tissue	Mild induration, able to move skin parallel to plane (sliding) and perpendicular to skin (pinching up)	Moderate induration, able to slide skin, unable to pinch skin; limiting instrumental ADL	Severe induration; unable to slide or pinch skin; limiting joint or orifice movement (e.g., mouth, anus); limiting self-care ADL	Generalized; associated with signs or symptoms of impaired breathing or feeding	Death
Wound dehiscence	Incisional separation of ≤25 % of wound, no deeper than superficial fascia	Incisional separation >25 % of wound with local care; asymptomatic hernia or symptomatic hernia without evidence of strangulation	Fascial disruption or dehiscence without evisceration; primary wound closure or revision by operative intervention indicated	Life-threatening consequences; symptomatic hernia with evidence of strangulation; fascial disruption with evisceration; major reconstruction flap, grafting, resection, or amputation indicated	Death
Wound infection	–	Localized; local intervention indicated (e.g., topical antibiotic, antifungal, or antiviral)	IV antibiotic, antifungal, or antiviral intervention indicated; radiologic or operative intervention indicated	Life-threatening consequences; urgent intervention indicated	Death
Postoperative hemorrhage	Minimal bleeding identified on clinical exam; intervention not indicated	Moderate bleeding; radiologic, endoscopic, or operative intervention indicated	Transfusion of ≥2 U (10 ml/kg for pediatrics) pRBCs beyond protocol specification indicated; urgent radiologic, endoscopic, or operative intervention indicated	Life-threatening consequences; urgent intervention indicated	Death
Soft tissue necrosis	–	Local wound care; medical intervention indicated (e.g., dressings or topical medications)	Operative debridement or other invasive intervention indicated (e.g., tissue reconstruction, flap or grafting)	Life-threatening consequences; urgent intervention indicated	Death
Pain	Mild pain	Moderate pain; limiting instrumental ADL	Severe pain; limiting self-care ADL	–	–

ADL activities of daily living, *pRBCs* packed red blood cells

temporarily over the disk to expose the correct portion of the breast to be irradiated with skin open. The target area for radiation was at least 2 cm from the margins. (5) The patient was transported from the operation suite to the radiation room. (6) Radiation (Clinac® 21EX, Varian Medical Systems, Inc.) at 21 Gy was delivered directly to the mammary gland. The cone is placed directly in contact with the breast target. The skin margins were gently stretched out of the radiation field to spare the skin from radiation damage. The energy of the electron beam ranged from 9 to 12 MeV. The correct collimator diameter was then selected and the optimal energy of the electron beam was selected on the basis of the thickness of irradiated breast tissue measured after the temporary reconstruction of the breast. The best dose distribution of radiotherapy in the gland is achieved if the thickness of the irradiated target remains as homogeneous as possible. Figure 1 shows the schema of simulated dose distribution in the case using a 12-MeV electric beam with a cone of 8 cm diameter. An acrylic resin bolus with 1 cm diameter is used to increase the surface dose distribution of the surgical bed. We also put a metallic plate at the deep edge of irradiated volume to minimize the dose to the chest wall and lung.

Results

From June 2011 to September 2011, 5 patients were enrolled in this pilot study and received 21 Gy. Follow-up ranged from 7.8 to 11.0 months (median 10.2). The patient characteristics are shown in Table 2. Patients were mostly elderly with smaller sized tumors and biologically lower risk (hormone receptor-positive and HER2-negative). Operation time ranged from 167 to 270 min (median 190 min) and intraoperative transportation to radiation room during the surgical procedure under general anesthesia was performed safely in all patients. The electron energy and collimator diameter used were 9 MeV (3 cases)

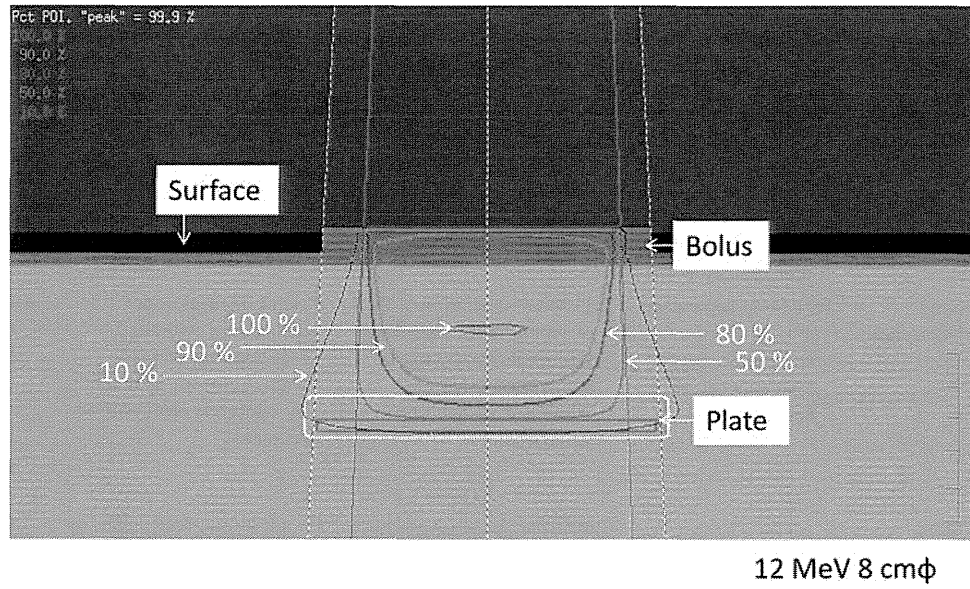

Fig. 1 Schema of simulated dose distribution in the case using a 12-MeV electric beam with a cone of 8 cm diameter. The surface indicates that of breast tissue. An acrylic resin bolus with 1 cm diameter is used to increase the surface dose distribution of the surgical bed. A metallic plate is put at the deep edge of the irradiated volume to minimize the dose to the chest wall and lung

Table 2 Patient characteristics ($n = 5$)

Characteristic	Number
Age (years)	
50–59	3
60–69	2
70+	0
Mean (range)	58.6 (52–68)
Tumor site	
Upper inner quadrant	2
Lower inner quadrant	1
Upper outer quadrant	2
Lower outer quadrant	0
Central portion	0
Tumor diameter (pathological tumor size)	
Tis	0
≤5 mm	0
>5 mm, ≤10 mm	1
>10 mm, ≤20 mm	4
>20 mm	0
Histology	
Ductal carcinoma in situ	0
Invasive ductal carcinoma	5
Tumor grade	
1	3
2	2
3	0
Hormone receptor status	
ER+ and/or PgR+	5
ER− and PgR−	0
HER2 status	
Positive	0
Negative	5

Table 3 Treatment-related toxicities (any grade) ($n = 5$)

Adverse event	Grade 1	Grade 2	Grade 3–5
Fibrosis deep connective tissue	3	0	0
Wound dehiscence	0	0	0
Wound infection	0	0	0
Postoperative hemorrhage	0	0	0
Soft tissue necrosis	0	0	0
Pain	3	0	0

and 12 MeV (2 cases), 8 cm (one case) and 6 cm (4 cases), respectively. The grading of main toxicities is shown in Table 3. Treatment-related toxicities within 3 months were deep connective tissue fibrosis (grade 1, $n = 3$) and pain (grade 1, $n = 3$). There was no case of wound infection, wound dehiscence, or soft tissue necrosis. Overall, there was no severe adverse event. All cases had negative margins on final pathology. To date, no local recurrence cases have been seen.

Discussion

This is a first report of a prospective single-center pilot study in a Japanese institution of IORT at a single dose of 21 Gy. The procedure required transportation of the patient under general anesthesia. We can conclude, as in another published Japanese phase I/II study [12, 13], that IORT requiring transportation is safe and manageable. Operation times ranged from 167 to 270 min (median 190), which showed that a longer time than that in the previous report is not needed [12]. However, the transport under general anesthesia needs to be carried out with careful observation.

As for PBI, the selection of patients is critical to its success [15, 16]. We now discuss the merits and limitations of IORT for early breast cancer. The main advantages of IORT are follows: (1) able to deliver the radiation before tumor cells have a chance to proliferate, which makes them more sensitive to the action of the radiation; (2) able to deliver radiation under direct visualization at the time of surgery and it has the potential for accurate dose delivery directly to the surgical bed; (3) able to minimize several side effects; since skin and the subcutaneous tissue can be spared, the radiation dose to lung and heart can be reduced; (4) able to achieve early initiation of radiation without delaying administration of chemotherapy; (5) able to decrease healthcare costs in some countries and the time required for outpatient treatment because one fraction is used; and (6) good cosmesis. Since the skin and the subcutaneous tissue are not irradiated, changes in breast appearance are not expected. This leads to a better cosmesis [17], although only a limited amount of data are available that evaluated late changes of cosmesis after IORT. The late cosmetic outcome is important for the evaluation of radiotherapy.

Limitations

Eligibility

Local recurrences after BCT with or without WBI arise mostly in the same quadrant as the primary cancer [18]. The main objective of radiotherapy after BCT is considered to be the destruction of residual cancer cells in the operative field. PBI administered around the tumor bed has been comparable to WBI in selected patients [19–22]. The risk factors for local recurrence after BCT are larger tumor size, higher tumor grade, younger age, lymph node-positive, and close surgical margin [3, 23, 24]. Clinical questions are then reviewed regarding which patients are suitable for IORT. Recommendations are shown for suitable patient groups selected for PBI outside of clinical trials (ASTRO Consensus Statement) in Table 4 [25]. Major points are discussed separately below.

Age

The cumulative incidence of tumor recurrence in the ispilateral breast after WBI with a boost is different with age, e.g., younger women have higher incidence [26]. Age at least 50 years has been selected in most prospective trials, and studies have shown that elderly patients treated with WBI [26, 27] or MammoSite® [28] were low risk. Few women younger than 50 years have been treated with PBI in prospective single-arm studies.

Tumor size

A maximum tumor size of 2 cm has been selected in most prospective trials. T2 tumors (>2 cm, ≤5 cm) or T0 tumors are recommended with caution [25]. Patients with T3 or T4 tumors should not receive PBI. An extensive intraductal

Table 4 Suitable patient group recommendation selections for APBI outside of clinical trials; ASTRO Consensus Statement [25]

Factors	Suitable group	Unsuitable group
Age (years)	≥60	<50
BRCA1/2 mutation	Not present	Present
Tumor size (cm)	≤2	>3
T stage	T1	T3 or T4
Margins	Negative by at least 2 mm	Positive
Grade	Any	NA
LVSI	No	Extensive
ER status	Positive	NA
Multicentricity	Unicentric only	If present
Multifocally	Clinically unifocal with total size ≤2 cm	If microscopically multifocal >3 cm in total size or if clinically multifocal
Histology	Invasive ductal or other favorable subtypes[a]	NA
Pure DCIS	Not allowed	If >3 cm in size
EIC	Not allowed	If >3 cm in size
Associated LCIS	Allowed	NA
Nodal status	pN0 (i−, i+)	pN1, pN2, pN3
Nodal surgery	SN Bx or ALND	None performed
Neoadjuvant therapy	Not allowed	If used

NA the given criteria are not applicable

[a] Favorable subtypes include mucinous, tubular, and colloid

component should be treated with caution. Patients with multicentric tumors, i.e., presence of tumor foci in different quadrants, should not receive PBI because of the extent of disease. Patients with clinically unifocal or multifocal tumors with a total tumor size no greater than 2 cm could be suitable for PBI [25].

Nodal status

Node-positive is one of the risk factors for ispilateral breast cancer [3]. Thus, the majority of patients who have been treated in prospective single-arm PBI trials had pathologically node-negative disease. Patients who do not undergo surgical nodal assessment or who have pathologic evidence of nodal involvements should not receive PBI.

Preoperative imaging

The ASTRO Task Force does not support the routine use of magnetic resonance imaging (MRI) in the APBI setting [29]. However, the detection of abnormalities outside the radiation field is important. MRI can identify multifocal and multicentric disease [30, 31]. Up to 16 % of abnormalities not found by mammograms or ultrasound can be detected by means of MRI [32], although MRI could not reduce the re-operation rate [33]. In patients treated with PBI, MRI should be strongly considered even if routine use is not recommended in the modern phase II or III studies [34].

Pathology

One area of concern in the use of IORT is the management of positive surgical margins as when positivity is discovered at the final histological examination a few days after surgery and IORT. Attention should be paid to ensure negative margins on final pathology [35], although margin positivity does not always influence the rate of local recurrences if effective radiotherapy is delivered [11, 36, 37]. Intraoperative frozen sections may be used to reduce positive margins [38]. Patients with close but negative margins (<2 mm) may be treated with caution [25]. Higher tumor grades are not suitable for PBI, because it is one of the risk factors for local recurrence and most prospective trials have not considered it as an eligibility criterion. HER2- or basal-type tumors have been shown to involve higher risk for local recurrence than luminal A or B types [11, 39, 40]. Thus, tailored local–regional treatment for early-stage breast cancer has now been reported to be mandatory [41].

Oncology

Only a few studies have been conducted of IORT including PBI in patients receiving neoadjuvant or concurrent chemotherapy. For patients who will receive adjuvant chemotherapy, it is recommended that PBI be performed first and followed by an interval of at least 2–3 weeks between completion of PBI and initiation of chemotherapy [25]. Thus, IORT including PBI allows radiotherapy to be given without delaying the administration of chemotherapy or hormonal therapy. A retrospective analysis from a MammoSite® registry single-arm trial reported an association between the initiation of adjuvant chemotherapy within 3 weeks of the last MammoSite® treatment and an increased risk of both radiation recall skin retraction and suboptimal cosmetics [42]. No data are available on when adjuvant endocrine therapy with PBI should be started.

Efficacy

The largest randomized clinical trial to date is now in progress at EIO. The goal of the trial is to compare the local recurrence rates between quadrantectomy with conventional WBI (60 Gy) and IORT (21 Gy) on overall survival. To date, the study remains investigational until information on long-term efficacy and safety becomes available [43]. In the trial at EIO, 21 Gy was used for the IORT arm. This dose was recommended after more than 1,000 IORT procedures [10]. In the most recent updated data (single arm), the local recurrence rate was 1.3 % (24/1,822) [11].

Safety

The most frequent early toxicity caused by WBI included pain, coloration of the skin, fatigue, and discomfort. Late toxicity included skin retraction and upper limb edema in the case of an irradiated axilla, and with less frequency rib osteitis, brachial plexopathy, and heart damage were encountered. With IORT, the overall incidence of early toxicity was less than 10 % [9], which included mild moderate effects (grade I or II) such as fibrosis, fat necrosis, edema, and erythema. With regard to late toxicity, there were few severe complications although a longer follow-up time is needed for evaluation [11]. Pulmonary fibrosis in patients treated with ELIOT is significantly less frequent compared to patients treated with WBI [44].

Conclusion

The first group of Japanese female patients tolerated the IORT procedure very well, as was the case with European women. A longer follow-up is needed for the evaluation of any potential late side effects or recurrences. A phase II study is now being conducted for the next group of patients (UMIN000003578). Careful management is needed

because selection of patients is critical to the successful application of IORT.

Acknowledgments This research was funded in part by the Japanese Foundation for Multidisciplinary Treatment of Cancer.

Conflict of interest The authors state that they have no conflict of interest.

References

1. Veronesi U, Cascinelli N, Mariani L, Greco M, Saccozzi R, Luini A, et al. Twenty-year follow-up of a randomized study comparing breast-conserving surgery with radical mastectomy for early breast cancer. N Engl J Med. 2002;347:1227–32.
2. Fisher B, Anderson S, Bryant J, Margolese RG, Deutsch M, Fisher ER, et al. Twenty-year follow-up of a randomized trial comparing total mastectomy, lumpectomy, and lumpectomy plus irradiation for the treatment of invasive breast cancer. N Engl J Med. 2002;347:1233–41.
3. Clarke M, Collins R, Darby S, Davies C, Elphinstone P, Evans E, et al. Effects of radiotherapy and of differences in the extent of surgery for early breast cancer on local recurrence and 15-year survival: an overview of the randomised trials. Lancet. 2005;366:2087–106.
4. Darby S, McGale P, Correa C, Taylor C, Arriagada R, Clarke M, et al. Effect of radiotherapy after breast-conserving surgery on 10-year recurrence and 15-year breast cancer death: meta-analysis of individual patient data for 10,801 women in 17 randomised trials. Lancet. 2011;378:1707–16.
5. Njeh CF, Saunders MW, Langton CM. Accelerated partial breast irradiation (APBI): a review of available techniques. Radiat Oncol. 2010;5.
6. Skandarajah AR, Lynch AC, Mackay JR, Ngan S, Heriot AG. The role of intraoperative radiotherapy in solid tumors. Ann Surg Oncol. 2009;16:735–44.
7. Veronesi U, Orecchia R, Luini A, Gatti G, Intra M, Zurrida S, et al. A preliminary report of intraoperative radiotherapy (IORT) in limited-stage breast cancers that are conservatively treated. Eur J Cancer. 2001;37:2178–83.
8. Luini A, Orecchia R, Gatti G, Intra M, Ciocca M, Galimberti V, et al. The pilot trial on intraoperative radiotherapy with electrons (ELIOT): update on the results. Breast Cancer Res Treat. 2005;93:55–9.
9. Veronesi U, Orecchia R, Luini A, Galimberti V, Gatti G, Intra M, et al. Full-dose intraoperative radiotherapy with electrons during breast-conserving surgery. Ann Surg. 2005;242:101–6.
10. Intra M, Luini A, Gatti G, Ciocca M, Gentilini O, Viana A, et al. Surgical technique of intraoperative radiation therapy with electrons (ELIOT) in breast cancer: a lesson learned by over 1000 procedures. Surgery. 2006;140:467–71.
11. Veronesi U, Orecchia R, Luini A, Galimberti V, Zurrida S, Intra M, et al. Intraoperative radiotherapy during breast conserving surgery: a study on 1,822 cases treated with electrons. Breast Cancer Res Treat. 2010;124:141–51.
12. Sawaki M, Sato S, Kikumori T, Ishihara S, Aoyama Y, Itoh Y, et al. A phase I study of intraoperative radiotherapy for early breast cancer in Japan. World J Surg. 2009;33:2587–92.
13. Sawaki M, Sato S, Noda S, Idota A, Uchida H, Tsunoda N, et al. Phase I/II study of intraoperative radiotherapy for early breast cancer in Japan. Breast Cancer. 2011. doi:10.1007/s12282-011-0294-1.
14. Oshima T, Aoyama Y, Shimozato T, Sawaki M, Imai T, Ito Y, et al. An experimental attenuation plate to improve the dose distribution in intraoperative electron beam radiotherapy for breast cancer. Phys Med Biol. 2009;54:3491–500.
15. Vicini F, Arthur D, Wazer D, Chen P, Mitchell C, Wallace M, et al. Limitations of the American Society of Therapeutic Radiology and Oncology Consensus Panel guidelines on the use of accelerated partial breast irradiation. Int J Radiat Oncol Biol Phys. 2011;79:977–84.
16. Polgár C, Limbergen EV, Pötter R, Kovács G, Polo A, Lyczek J, et al. Patient selection for accelerated partial-breast irradiation (APBI) after breast-conserving surgery: recommendations of the Groupe Européen de Curiethérapie-European Society for Therapeutic Radiology and Oncology (GEC-ESTRO) breast cancer working group based on clinical evidence (2009). Radiother Oncol. 2010;94:264–73.
17. Orecchia R, Ivaldi GB, Leonardi MC. Integrated breast conservation and intraoperative radiation therapy. Breast. 2009;18(Suppl 3):S98–102.
18. Veronesi U, Marubini E, Mariani L, Galimberti V, Luini A, Veronesi P, et al. Radiotherapy after breast-conserving surgery in small breast carcinoma: long-term results of a randomized trial. Ann Oncol. 2001;12:997–1003.
19. Vicini FA, Kestin L, Chen P, Benitez P, Goldstein NS, Martinez A. Limited-field radiation therapy in the management of early-stage breast cancer. JNCI J Nat Cancer Inst. 2003;95:1205–10.
20. Benitez P, Keisch M, Vicini F, Stolier A, Scroggins T, Walker A, et al. Five-year results: the initial clinical trial of Mammosite balloon brachytherapy for partial breast irradiation in early-stage breast cancer. Am J Surg. 2007;194:456–62.
21. Vicini FA, Baglan KL, Kestin LL, Mitchell C, Chen PY, Frazier RC, et al. Accelerated treatment of breast cancer. J Clin Oncol. 2001;19:1993–2001.
22. Antonucci JV, Wallace M, Goldstein NS, Kestin L, Chen P, Benitez P, et al. Differences in patterns of failure in patients treated with accelerated partial breast irradiation versus whole-breast irradiation: a matched-pair analysis with 10-year follow-up. Int J Radiat Oncol Biol Phys. 2009;74:447–52.
23. Park CC, Mitsumori M, Nixon A, Recht A, Connolly J, Gelman R, et al. Outcome at 8 years after breast-conserving surgery and radiation therapy for invasive breast cancer: influence of margin status and systemic therapy on local recurrence. J Clin Oncol. 2000;18:1668–75.
24. Fisher ER. Lumpectomy margins and much more. Cancer. 1997;79:1453–8 (discussion 9–60).
25. Smith BD, Arthur DW, Buchholz TA, Haffty BG, Hahn CA, Hardenbergh PH, et al. Accelerated partial breast irradiation consensus statement from the American Society for Radiation Oncology (ASTRO). J Am Coll Surg. 2009;209:269–77.
26. Bartelink H, Horiot JC, Poortmans PM, Struikmans H, Van den Bogaert W, Fourquet A, et al. Impact of a higher radiation dose on local control and survival in breast-conserving therapy of early breast cancer: 10-year results of the randomized boost versus no boost EORTC 22881-10882 trial. J Clin Oncol. 2007;25:3259–65.
27. Antonini N, Jones H, Horiot JC, Poortmans P, Struikmans H, Van den Bogaert W, et al. Effect of age and radiation dose on local control after breast conserving treatment: EORTC trial 22881-10882. Radiother Oncol. 2007;82:265–71.
28. Chao KK, Vicini FA, Wallace M, Mitchell C, Chen P, Ghilezan M, et al. Analysis of treatment efficacy, cosmesis, and toxicity using the MammoSite breast brachytherapy catheter to deliver accelerated partial-breast irradiation: the William Beaumont Hospital experience. Int J Radiat Oncol Biol Phys. 2007;69:32–40.

29. Smith BD, Arthur DW, Buchholz TA, Haffty BG, Hahn CA, Hardenbergh PH, et al. Accelerated partial breast irradiation consensus statement from the American Society for Radiation Oncology (ASTRO). Int J Radiat Oncol Biol Phys. 2009;74:987–1001.
30. Al-Hallaq HA, Mell LK, Bradley JA, Chen LF, Ali AN, Weichselbaum RR, et al. Magnetic resonance imaging identifies multifocal and multicentric disease in breast cancer patients who are eligible for partial breast irradiation. Cancer. 2008;113:2408–14.
31. Tendulkar RD, Chellman-Jeffers M, Rybicki LA, Rim A, Kotwal A, Macklis R, et al. Preoperative breast magnetic resonance imaging in early breast cancer: implications for partial breast irradiation. Cancer. 2009;115:1621–30.
32. Houssami N, Ciatto S, Macaskill P, Lord SJ, Warren RM, Dixon JM, et al. Accuracy and surgical impact of magnetic resonance imaging in breast cancer staging: systematic review and meta-analysis in detection of multifocal and multicentric cancer. J Clin Oncol. 2008;26:3248–58.
33. Turnbull L, Brown S, Harvey I, Olivier C, Drew P, Napp V, et al. Comparative effectiveness of MRI in breast cancer (COMICE) trial: a randomised controlled trial. Lancet. 2010;375:563–71.
34. Orecchia R, Leonardo MC. Intraoperative radiation therapy: is it a standard now? Breast. 2011;20(Suppl 3):S111–5.
35. Beal K, McCormick B, Zelefsky M, Borgen P, Fey J, Goldberg J, et al. Single-fraction intraoperative radiotherapy for breast cancer: early cosmetic results. Int J Radiat Oncol Biol Phys. 2007;69:19–24.
36. Chism D, Freedman G, Li T, Anderson P. Re-excision of margins before breast radiation—diagnostic or therapeutic? Int J Radiat Oncol Biol Phys. 2006;65:1416–21.
37. Mariani L, Salvadori B, Marubini E, Conti AR, Rovini D, Cusumano F, et al. Ten year results of a randomised trial comparing two conservative treatment strategies for small size breast cancer. Eur J Cancer. 1998;34:1156–62.
38. Fukamachi K, Ishida T, Usami S, Takeda M, Watanabe M, Sasano H, et al. Total-circumference intraoperative frozen section analysis reduces margin-positive rate in breast-conservation surgery. Jpn J Clin Oncol. 2010;40:513–20.
39. Kyndi M, Sorensen FB, Knudsen H, Overgaard M, Nielsen HM, Overgaard J. Estrogen receptor, progesterone receptor, HER-2, and response to postmastectomy radiotherapy in high-risk breast cancer: the Danish Breast Cancer Cooperative Group. J Clin Oncol. 2008;26:1419–26.
40. Nguyen PL, Taghian AG, Katz MS, Niemierko A, Abi Raad RF, Boon WL, et al. Breast cancer subtype approximated by estrogen receptor, progesterone receptor, and HER-2 is associated with local and distant recurrence after breast-conserving therapy. J Clin Oncol. 2008;26:2373–8.
41. Solin LJ. Tailored local-regional treatment for early-stage breast cancer. Clin Breast Cancer. 2010;10:343–4.
42. Haffty BG, Vicini FA, Beitsch P, Quiet C, Keleher A, Garcia D, et al. Timing of chemotherapy after MammoSite radiation therapy system breast brachytherapy: analysis of the American Society of Breast Surgeons MammoSite breast brachytherapy registry trial. Int J Radiat Oncol Biol Phys. 2008;72:1441–8.
43. Buchholz TA. Radiation therapy for early-stage breast cancer after breast-conserving surgery. N Engl J Med. 2009;360:63–70.
44. Rampinelli C, Bellomi M, Ivaldi GB, Intra M, Raimondi S, Meroni S, et al. Assessment of pulmonary fibrosis after radiotherapy (RT) in breast conserving surgery: comparison between conventional external beam RT (EBRT) and intraoperative RT with electrons (ELIOT). Technol Cancer Res Treat. 2011;10:323–9.

J. Radiat. Res., 53, 138–144 (2012)

Evaluation of Parotid Gland Function using Equivalent Cross-relaxation Rate Imaging Applied Magnetization Transfer Effect

Hidetoshi SHIMIZU[1]*, Shigeru MATSUSHIMA[2], Yasutomi KINOSADA[3], Hiroki MIYAMURA[2], Natsuo TOMITA[1], Takashi KUBOTA[1], Hikaru OSAKI[1], Masashi NAKAYAMA[1], Manabu YOSHIMOTO[1] and Takeshi KODAIRA[1]

Radiotherapy/Function/ECRI/Scintigraphy/Parotid gland.

Safe imaging modalities are needed for evaluating parotid gland function. The aim of this study was to validate the utility of a magnetic resonance imaging (MRI) tool, equivalent cross-relaxation rate imaging (ECRI), as a measurement of parotid gland function after chemoradiotherapy. Subjects comprised 18 patients with head-neck cancer who underwent ECRI and salivary gland scintigraphy. First, we calculated ECR values (signal intensity on ECRI), maximum uptake rate (MUR) and washout rate (WOR) from salivary gland scintigraphy data at the parotid glands. Second, we investigated correlations between ECR values and each parameter of MUR (uptake function) and WOR (secretory function) obtained by salivary gland scintigraphy at the parotid gland. Next, we investigated each dose-response for ECR, MUR and WOR at the parotid gland. A correlation was detected between ECR values and MUR in both the pre- ($r = -0.55$, $p < 0.01$) and post-treatment ($r = -0.50$, $p < 0.05$) groups. A significant post-treatment correlation was detected between the percentage change in ECR values at 3–5 months after chemoradiotherapy and median dose to the parotid gland (Pearson correlation, $r = -0.62$, $p < 0.05$). However, no correlations were detected between median dose to the parotid gland and either MUR or WOR. ECRI is a new imaging tool for evaluating the uptake function of the parotid gland after chemoradiotherapy.

INTRODUCTION

Radiotherapy for head and neck cancers must be performed with care, as various high-risk organs are situated in the surrounding area. Decreasing side effects in these organs is thus problematic. The parotid gland shows high radiosensitivity and inclusion within the irradiation field during radiotherapy for head and neck cancer causes depression of parotid gland function. Evaluation of parotid gland function after radiotherapy has been performed using salivary gland scintigraphy.[1–3] This modality can evaluate parotid gland function by observing the movement of radionuclide ($^{99m}TcO_4^-$) that accumulates in the parotid gland. However, the use of radionuclides obviously means that radiation exposure for human bodies is unavoidable,[4] making this technique unsuitable for regular evaluation of parotid gland depression caused by radiotherapy.

Magnetic resonance imaging (MRI) uses magnetism and electromagnetic waves, representing a noninvasive modality with no exposure to radiation. The apparent diffusion coefficient (ADC) obtained by diffusion-weighted imaging has been reported as a parameter for evaluating parotid function.[5–7] However, ADC shows a low correlation coefficient with the function parameter obtained by salivary gland scintigraphy.[7]

We selected equivalent cross-relaxation rate imaging (ECRI) applied magnetization transfer effect using MRI.[8–12] ECRI can detect minute changes in organization and molecular structure, offering information reflecting interactions with water molecules and biomacromolecules.[8]

The aim of the present study was to validate the utility of ECRI for evaluating parotid gland function after chemoradiotherapy. ECRI provides difference information for parts irradiated with a single saturation pulse. ECRI can obtain cell-density-weighted images and fiber-density-weighted images by irradiating a saturation pulse close to or far from the center frequency of water, respectively.[10,12] The acinar

*Corresponding author: Phone: +81-52-762-6111,
Fax: +81-52-752-8390,
E-mail: hishimizu@aichi-co.jp

[1]Department of Therapeutic Radiation Oncology, Aichi Cancer Center Hospital, 1-1 Kanokoden, Chikusa-ku, Nagoya 464-8681, Japan; [2]Department of Diagnostic and Interventional Radiology, Aichi Cancer Center Hospital, 1-1 Kanokoden, Chikusa-ku, Nagoya 464-8681, Japan; [3]Department of Biomedical Informatics, Gifu University Graduate School of Medicine, 1-1 Yanagido, Gifu 501-1193, Japan.
doi:10.1269/jrr.11059

cell composing the parotid gland plays a big role to the uptake of saliva. Therefore, we irradiated with a saturation pulse at 7 ppm downfield from the center frequency of water to obtain cell-density-weighted images in this research. We first investigated correlations between ECR values (signal intensity on ECRI) at the parotid gland and parameters (uptake function and secretory function) as obtained by salivary gland scintigraphy. We then investigated each dose-response for ECR and salivary gland scintigraphy parameters in the parotid gland.

MATERIALS AND METHODS

Patients

Subjects comprised 18 patients with head and neck cancer. Table 1 shows patient characteristics. Disease was staged according to the American Joint Committee on Cancer 1997 clinical staging.[13] All patients received an explanation about the purpose and methods of this research and issues related to the protection of privacy, and informed consent to participate in the study was obtained prior to enrolment. MRI and salivary gland scintigraphy were performed in 6 patients before chemoradiotherapy, 6 patients after chemoradiotherapy and 6 patients both before and after chemoradiotherapy. As a result, 24 series of data were obtained for 48 parotid glands.

Chemoradiotherapy

All patients were immobilized in a cast, and computed tomography (CT) with 2.5 mm slice thickness was taken for treatment planning. Scans included the target area, regional lymph nodes, and the parotid glands. Target objects and normal structures including both parotid glands were contoured on a Pinnacle workstation (Hitachi Medical Corporation, Tokyo, Japan). Computed tomography (CT) images with the contour objects were transferred to a specific treatment planning system (Tomoprovider; TomoTherapy, Madison, WI).

Table 1. Patient characteristics

N	18
Male/female	15/3
Median age (range)	53 (16–74)
Tumor site	
Nasopharynx	16
Oropharynx	2
Stage	
I	1 (6%)
II	2 (11%)
III	8 (44%)
IV	7 (39%)

A dose of 66–70 Gy was prescribed to the primary tumor. Most patients were treated using a fractionation scheme with 2 Gy administered 5 times/week. One patient received 1.8 Gy per fraction. Dose constraints for parotid glands were mean dose < 30 Gy, median < 23 Gy and whole parotid gland volume with < 20 Gy > 20 mm^3. Other planning parameters comprised: primary collimator width, 2.5 cm; pitch, 0.3; and modulation factor, 3.0–4.0.

Radiotherapy was performed using a Hi-ART System (TomoTherapy), which is specifically designed for intensity-modulated radiotherapy (IMRT). All patients received daily megavoltage CT (MVCT) acquisitions for setup verification.[14,15]

Chemotherapy was planned for 16 patients, with only 2 patient undergoing radiotherapy alone, as medical condition was considered insufficient for systemic chemotherapy. Three courses of chemotherapy comprising continuous intravenous administration of 5-fluorouracil at 800 mg/m^2/24 h for 5 days (Days 1–5) and nedaplatin (NDP) at 130 mg/m^2/6 h for 1 day (Day 6) were administered approximately every 4 weeks in the alternating setting. The details of contents of chemoradiotherapy have been reported in other articles.[16]

Imaging techniques

Salivary gland scintigraphy was performed before initial treatment and then 3–5 months after completion of chemoradiotherapy. Salivary gland scintigraphy was performed with the gamma camera from a MillenniumVG system (GE Yokokawa Medical System, Milwaukee, WI). The only restriction before the examination was a dietary restriction. Dynamic imaging was obtained in a 64 × 64 pixel matrix at 15 s per frame for 45 min immediately after intravenous injection of 370 MBq of $^{99m}TcO_4^-$. Lemon juice (0.5 ml) was dripped into the oral cavity in 1800 s after intravenous injection as a taste stimulus. The energy window was ±10% around the 140 keV photopeak of ^{99m}Tc.

MRI was scheduled before initial treatment and then 3–5 months after completion of chemoradiotherapy. A 1.5-T system (Signa; GE Yokokawa Medical System) was used. Sequences comprised 3-dimensional spoiled gradient recalled acquisition in the steady state (3DSPGR) and saturation-transfer-prepared 3DSPGR (ST-3DSPGR). Single saturation transfer pulse (3.26 μT) frequency was employed at the frequency of 7 ppm downfield from the center frequency of water. Scans included the whole parotid gland. A neurovascular coil was used. Conditions were: repetition time, 40 ms; echo time, 6.9 ms; flip angle, 30°; bandwidth, 15.63 kHz; field of view, 24 cm; slice thickness, 5 mm; overlap locations, 0; locations per slab, 16; acquisition matrix, 512 × 126; and reconstructed matrix size, 512 × 512 (zerofill interoperation process). The stimulation of the parotid gland by for example lemon juice was not performed as in the scintigraphy protocol during MRI.

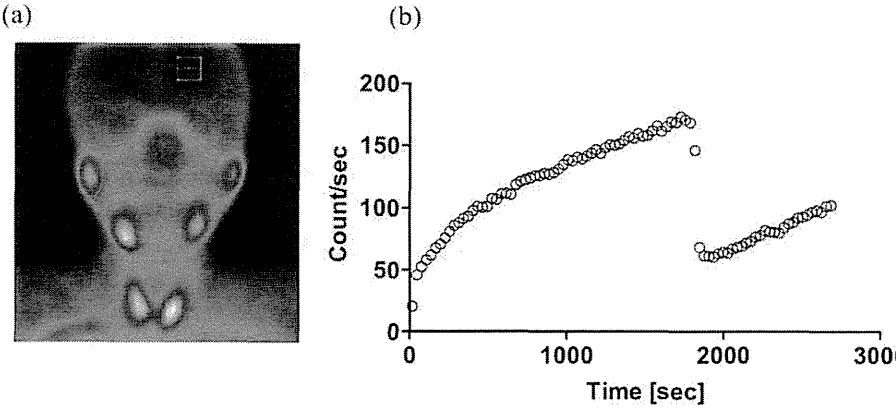

Fig. 1. (**a**) Planar image taken by salivary gland scintigraphy. ROIs were located for bilateral parotid glands and a frontal sinus. The count for the frontal sinus was used as the background level. (**b**) Representative time-activity curve (TAC) on a parotid gland. TAC on the parotid gland was created by subtracting background from the count for the gland.

Data analysis

Regions of interest (ROIs) were located for bilateral parotid glands and a frontal sinus on the planar image obtained by salivary gland scintigraphy (Fig. 1a), using the count for the frontal sinus as the background signal. A time-activity curve (TAC) for the parotid gland was created by subtracting the background from the count for the parotid gland (Fig. 1b). Maximum uptake rate (MUR) was calculated for bilateral parotid glands according to Equation 1.

$$MUR = (1 - C_{vpp} / C_{max}) \times 100\ [\%] \quad (1)$$

where C_{vpp} is the count on TAC at 60 s after administration of $^{99m}TcO_4^-$ (reflecting blood flow, capillary permeability and secretion rate in the parotid gland) and C_{max} is the maximum count on the TAC (reflecting capacities of blood vessel lumens and intercellular spaces in the parotid gland). MUR was used as the parameter indicating uptake function.

Washout rate (WOR) was calculated for bilateral parotid glands according to Equation 2.

$$WOR = (1 - C_{min} / C_{max}) \times 100\ [\%] \quad (2)$$

where C_{min} is the minimum counts after taste stimulation. WOR thus shows the secretion of $^{99m}TcO_4^-$ per capacities of blood vessel lumens and intercellular spaces in the parotid gland. WOR was used as the parameter indicating secretory function.

ECRI was obtained using Equation 3.

$$ECR = (M_0 / Ms - 1) \times 100\ [\%] \quad (3)$$

where Ms and M_0 represent signal intensities in 3DSPGR and ST-3DSPGR images, respectively. A ROI was located for the parotid gland on ECRI, and ECR at the parotid gland was measured.

We investigated correlations between ECR and both MUR and WOR at the parotid gland before and after chemoradiotherapy. Next, we investigated simple linear correlations between percentage changes in ECR, MUR and WOR at 3–5 months after chemoradiotherapy and median dose to the parotid gland.

Table 2. Changes in parameters

(a)

	Pre treatment series group (No. of parotid glands = 24)		Post treatment series group (No. of parotid glands = 24)
MUR	74.7 ± 10.8	***	59.7 ± 8.1
WOR	61.0 ± 9.6	***	21.0 ± 16.5

(b)

ECR values	30.0 ± 19.9	***	53.3 ± 22.5

Student's t test *** $p < 0.001$

Statistical analysis

R2.5.1 statistical software (www.r-project.org/) was used to perform all analyses. Student's t test was used to compare differences in patient groups. Pearson's correlation was used to evaluate correlations between ECR and MUR and between ECR and WOR at the parotid gland, and between percentage changes in ECR, MUR and WOR at 3–5 months after chemoradiotherapy and median dose to the parotid gland. The level of significance was set at 5%, and all p values were based on two-tailed tests.

RESULTS

Findings from salivary gland scintigraphy

Planar images taken by salivary gland scintigraphy were obtained in all cases without any acquisition failure. MUR and WOR could be obtained from all parotid glands on planar images. Table 2a shows changes in MUR and WOR

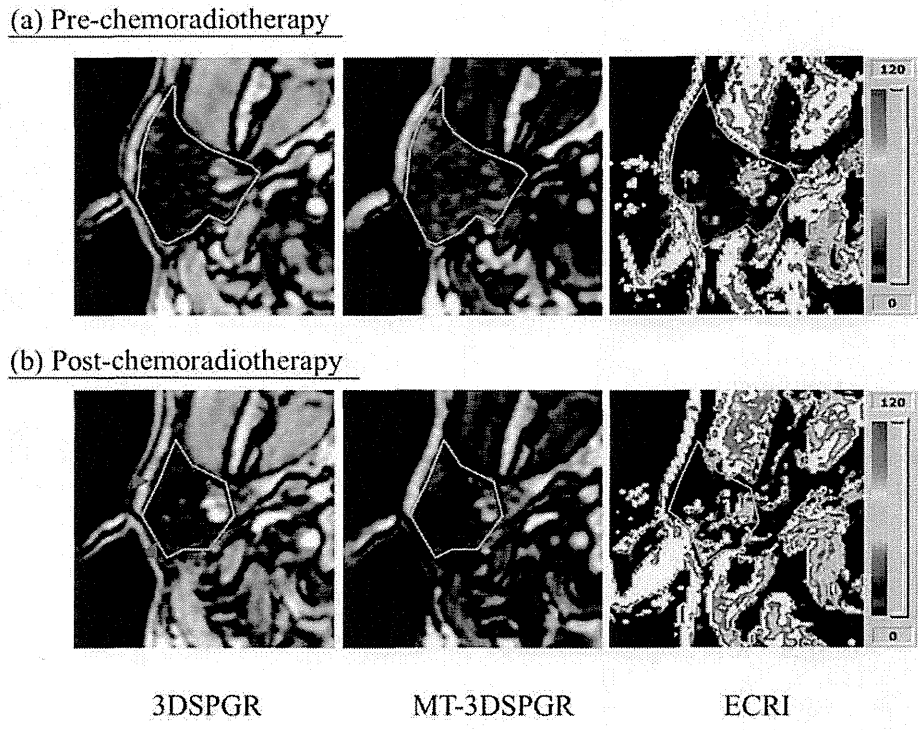

Fig. 2. Examples of 3DSPGR, MT-3DSPGR and ECR before (**a**) and after (**b**) chemoradiotherapy. Right parotid glands (areas surrounded by the yellow line) are shown in the axial plane. Volume reduction (indicated by arrowhead) was detected after chemoradiotherapy. ECRI was obtained using Equation 3.

between pre- and post-treatment groups. MUR was lower in the post-treatment group than in the pre-treatment group (Student's t test, $p < 0.001$). WOR was also lower in the post-treatment group than in the pre-treatment group (Student's t test, $p < 0.001$). Losses of uptake and secretory function in the parotid gland were thus confirmed by salivary gland scintigraphy.

Findings from ECRI

Both 3DSPGR and MT-3DSPGR images were obtained in all cases without any acquisition failure. ECR images were obtained using Equation 3. Figure 2 shows examples of 3DSPGR, MT-3DSPGR and ECR images before and after chemoradiotherapy. A clear reduction in parotid gland size after chemoradiotherapy was detected in this representative case (Fig. 2, arrowhead). ECR images were expressed in a graded color diagram of ECR values ranging from 0 to 120, with red indicating areas of high ECR, black showing areas of low ECR, and white representing areas with ECR > 120. Mean ECR values at parotid glands (± standard deviation) were 14.2 ± 0.72% and 34.3 ± 0.70% before and after chemoradiotherapy, respectively (Fig. 2). ECR values were higher in the post-treatment group than in the pre-treatment group (Table 2b; Student's t test, $p < 0.001$).

Correlations between ECR value and salivary gland scintigraphy parameters

To determine whether ECR values can be used to evaluate parotid gland function, we investigated correlations between ECR value and salivary gland scintigraphy parameters at the parotid gland. The correlation coefficient between ECR and MUR was –0.55 in the pre-treatment group (Pearson correlation, $p < 0.01$) and –0.50 in the post-treatment group (Pearson correlation, $p < 0.05$) (Fig. 3a). The correlation coefficients between ECR and WOR were –0.32 in the pre-treatment group (Pearson correlation, $p = 0.12$) and –0.06 in the post-treatment group (Pearson correlation, $p = 0.79$) (Fig. 3b).

Dose response

The 6 patients who underwent salivary gland scintigraphy and MRI both before and after chemoradiotherapy received a median dose of 19.8–26.5 Gy to the parotid glands (Table 3). The doses (several cGy per a MVCT acquisition) from the MVCT imaging were not contained in the median dose. Figure 4 shows the correlation between percentage change in parameters and median dose to the parotid gland. A significant correlation was identified between percentage change in ECR value at 3–5 months after chemoradiotherapy and median dose to the parotid gland (Pearson correlation, $r = -0.62$, $p < 0.05$). The correlation between percentage change

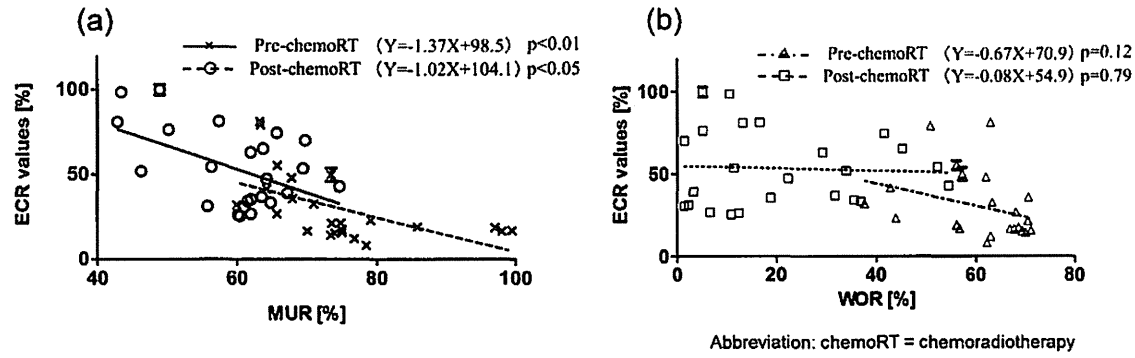

Fig. 3. Relationships between ECR value and salivary gland scintigraphy parameters. (a) MUR; (b) WOR.

Table 3. Median dose to parotid glands [Gy]

Patient No.	Right	Left
1	26.5	24.5
2	22.3	21.8
3	26.0	24.7
4	19.8	20.3
5	22.7	21.2
6	20.1	20.5

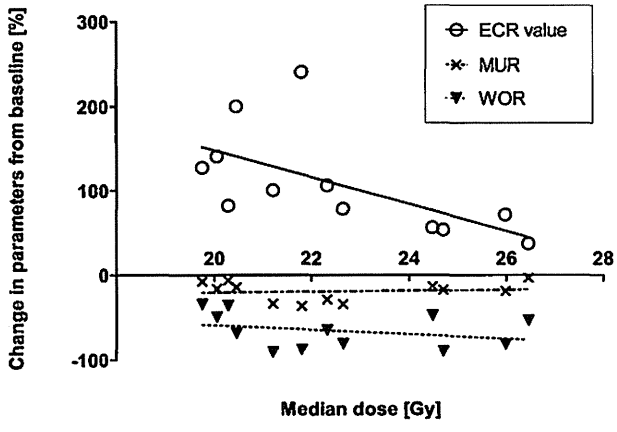

Fig. 4. Correlations between percentage change in parameters from baseline and median dose to parotid glands.

in MUR at 3–5 months after chemoradiotherapy and median dose to the parotid gland was not significant (Pearson correlation, $r = 0.11$, $p = 0.74$). The correlation between percentage change in WOR at 3–5 months after chemoradiotherapy and median dose to the parotid gland was also not significant (Pearson correlation, $r = -0.31$, $p = 0.33$).

DISCUSSION

Matsushima *et al.* previously reported ECRI as a potentially useful method for evaluating the efficacy of sentinel lymph node biopsy[9,10] and for cellular density imaging of axillary lymph nodes.[11] Yuen *et al.* reported ECRI as a feasible imaging technique for demonstrating breast cancer.[12] ECRI can thus detect minute changes in molecular and organizational structure.[8]

The present study represents the first trial of evaluating parotid gland function after chemoradiotherapy using ECRI. Parotid gland evaluation by MRI has been reported using ADC, which detects the motion of water molecules and microcirculatory blood flow.[5–7] Theony *et al.* reported that ADC value decreased immediately after taste stimulation, then increased until static state.[5] Dirix *et al.* reported that ADC value decreased significantly after irradiation.[6] Likewise, Lin *et al.* reported that ADC value decreased significantly after irradiation, and correlated with parameters obtained by salivary scintigraphy (uptake rate; $r = 0.36$, $p < 0.01$, MUR; $r = 0.33$, $p < 0.01$).[7] In our results, correlation coefficients between ECR and MUR were –0.55 ($p < 0.01$) in the pre-treatment group and –0.50 ($p < 0.05$) in the post-treatment group. The correlation coefficient between ECR and MUR was higher than that between ADC and MUR in past studies.[7] The reason why ECR correlated with MUR before chemoradiotherapy is as follows. When capacities of blood vessel lumens and intercellular spaces are large, C_{vpp} / C_{max} is low, and MUR (defined as $1 - C_{vpp} / C_{max}$) is high. Conversely, cell densities are relatively decreased, and the ECR (expressing cell density) is thus low. ECR thus showed a negative correlation with MUR. Moreover, ECR showed a correlation with MUR in the post-treatment group for the following reasons. Animal experiments have identified shrinkage of irradiated parotid glands.[17] Likewise, the parotid gland after chemoradiotherapy shrank in the present study (Fig. 2). ECR shows a high value due to the rise in cell density, while MUR was low due to decreased free water and the narrowness of the free water division, with shrinkage of gland tissues. ECR therefore shows a negative correlation with MUR in the post-treatment group. This relationship suggests that ECR value can be used to evaluate uptake function of the parotid gland after chemoradiotherapy without exposure to radiation. In addition, as ECRI can provide

a 2-dimensional color map (Fig. 2), areas of weak uptake function in the parotid gland can be identified visually. The details of mechanism for the uptake of saliva are unknown. Therefore, the visualization of uptake function may contribute for the clarification of the loss part of uptake function of saliva. The correlation coefficients between ECR and WOR were –0.32 in the pre-treatment group (Pearson correlation, $p = 0.12$) and –0.06 in the post-treatment group (Pearson correlation, $p = 0.79$) (Fig. 3b). However, as the stimulation of the parotid gland by for example lemon juice was not performed as in the scintigraphy protocol during MRI, both exams could not be compared.

On salivary scintigraphy, dose-response with parotid gland function has been studied by other investigators,[1–3,18–20] Roesink *et al.* found a significant correlation between salivary excretion factor (defined as the percentage of activity in the parotid gland that disappeared within 15 min following administration of carbachol) and mean radiation dose to the parotid glands.[3] However, in our research, WOR did not show a linear correlation with radiation dose to the parotid glands (Fig. 4). This lack of correlation may be due to low number of patients and differences in dose ranges applied in this study. Moreover, the difference between median and mean doses might be involved. On the other hand, calculations of secretory functions (such as salivary excretion factor and WOR) and uptake functions (such as MUR) have been widely recognized for salivary scintigraphy. However, dose-response for uptake function has not been reported. In our research, the percentage change in MUR at 3–5 months after chemoradiotherapy did not show a linear correlation with median radiation dose to the parotid gland (Pearson correlation, $r = 0.11$, $p = 0.74$). Conversely, the percentage change in ECR values at 3–5 months after chemoradiotherapy showed a linear correlation with median radiation dose to the parotid gland (Pearson correlation, $r = -0.62$, $p < 0.05$). ECR thus showed a linear correlation with median radiation dose to parotid glands in the range of 19.8–26.5 Gy. The reason why ECR correlates with median radiation dose to the parotid gland can be described as follows from the perspective of cell density. In this research, cell-density-weighted images were obtained by irradiating the saturation pulse at a frequency 7 ppm downfield from the center frequency of water. Matsushima *et al.* reported that ECR correlated with cell density in clinical situations.[11] In addition, the number of acinar cells is known to be decreased in irradiated salivary gland.[21–27] Li *et al.* reported that the number of acinar cells in irradiated parotid glands was decreased at 16 weeks after radiotherapy.[27] This duration after radiotherapy is similar to that used in our research. Loss of acinar cells is markedly increased with increasing dose to the parotid gland.[26,27] The percentage change in ECR values at 3–5 months after chemoradiotherapy thus shows a clear inverse correlation with median radiation dose to the parotid gland. This suggests that ECR value can be used to predict uptake function of the parotid gland after chemoradiotherapy.

In conclusion, we verified that ECRI is useful for evaluating parotid gland function after chemoradiotherapy. ECRI allowed visual evaluation of uptake function in the parotid gland without exposure to radiation.

ACKNOWLEDGEMENTS

We are indebted to Masataka Murakami at National Institute for Physiological Sciences and Seiichi Era at Gifu University Graduate School of Medicine for many helpful discussions in the course of this investigation.

REFERENCES

1. Munter MW, *et al* (2007) Changes in salivary gland function after radiotherapy of head and neck tumors measured by quantitative pertechnetate scintigraphy: comparison of intensity-modulated radiotherapy and conventional radiation therapy with and without Amifostine. Int J Radiat Oncol Biol Phys **67**(3): 651–659.
2. Bussels B, *et al* (2004) Dose-response relationships within the parotid gland after radiotherapy for head and neck cancer. Radiother Oncol **73**(3): 297–306.
3. Roesink JM, *et al* (2004) Scintigraphic assessment of early and late parotid gland function after radiotherapy for head-and-neck cancer: a prospective study of dose-volume response relationships. Int J Radiat Oncol Biol Phys **58**(5): 1451–1460.
4. ICRP Publication 53 (1987) Radiation dose to patients from radiopharmaceuticals.
5. Thoeny HC, *et al* (2005) Gustatory stimulation changes the apparent diffusion coefficient of salivary glands: initial experience. Radiology **235**(2): 629–634.
6. Dirix P, *et al* (2008) Diffusion-weighted magnetic resonance imaging to evaluate major salivary gland function before and after radiotherapy. Int J Radiat Oncol Biol Phys **71**(5): 1365–1371.
7. Zhang L, *et al* (2001) Yoshimura R, Shibuya H. Functional evaluation with intravoxel incoherent motion echo-planar MRI in irradiated salivary glands: a correlative study with salivary gland scintigraphy. J Magn Reson Imaging **14**(3): 223–229.
8. Sogami M, *et al* (2001) Basic studies on the equivalent cross-relaxation rate imaging (equivalent CRI)--phantom studies. NMR Biomed **14**(6): 367–375.
9. Matsushima S, *et al* (2005) Equivalent cross-relaxation rate imaging for sentinel lymph node biopsy in breast carcinoma. Magn Reson Med **54**(5): 1300–1304.
10. Matsushima S, *et al* (2003) Equivalent cross relaxation rate image for decreasing a false negative case of sentinel lymph node biopsy. Magn Reson Imaging **21**(9): 1045–1047.
11. Mastsushima S, *et al* (2008) Equivalent cross-relaxation rate imaging of axillary lymph nodes in breast cancer. J Magn Reson Imaging **27**(6): 1278–1283.
12. Yuen S, *et al* (2004) Equivalent cross-relaxation rate imaging of breast cancer. J Magn Reson Imaging **20**(1): 56–65.
13. Fleming ID, Cooper JS and Henson DE (1997) AJCC cancer staging manual. 5th ed. Philadelphia: J. B. Lippincott.

14. Forrest LJ, *et al* (2004) The utility of megavoltage computed tomography images from a helical tomotherapy system for setup verification purposes. Int J Radiat Oncol Biol Phys **60**(5): 1639–1644.
15. Langen KM, *et al* (2005). Initial experience with megavoltage (MV) CT guidance for daily prostate alignments. Int J Radiat Oncol Biol Phys **62**(5): 1517–1524.
16. Fuwa N, *et al* (2002) Phase I study of combination chemotherapy with 5-fluorouracil (5-FU) and nedaplatin (NDP): adverse effects and eecommended dose of NDP administered after 5-FU. Am J Clin Oncol **25**(6): 565–569.
17. Vasquez Osorio EM, *et al* (2008) Local anatomic changes in parotid and submandibular glands during radiotherapy for oropharynx cancer and correlation with dose, studied in detail with nonrigid registration. Int J Radiat Oncol Biol Phys **70**(3): 875–882.
18. van Acker F, *et al* (2001) The utility of SPECT in determining the relationship between radiation dose and salivary gland dysfunction after radiotherapy. Nucl Med Commun **22**(2): 225–231.
19. Tenhunen M, *et al* (2008) Scintigraphy in prediction of the salivary gland function after gland-sparing intensity modulated radiation therapy for head and neck cancer. Radiother Oncol **87**(2): 260–267.
20. Maes A, *et al* (2002) Preservation of parotid function with uncomplicated conformal radiotherapy. Radiother Oncol **63**(2): 203–211.
21. Price RE, *et al* (1995) Effects of continuous hyperfractionated accelerated and conventionally fractionated radiotherapy on the parotid and submandibular salivary glands of rhesus monkeys. Radiother Oncol **34**(1): 39–46.
22. Coppes RP, Vissink A and Konings AW (2002) Comparison of radiosensitivity of rat parotid and submandibular glands after different radiation schedules. Radiother Oncol **63**(3): 321–328.
23. Urek MM, *et al* (2005) Early and late effects of X-irradiation on submandibular gland: a morphological study in mice. Arch Med Res **36**(4): 339–343.
24. Cooper JS, *et al* (1995) Late effects of radiation therapy in the head and neck region. Int J Radiat Oncol Biol Phys **31**(5): 1141–1164.
25. Konings AW, Coppes RP and Vissink A (2005) On the mechanism of salivary gland radiosensitivity. Int J Radiat Oncol Biol Phys **62**(4): 1187–1194.
26. Muhvic-Urek M, *et al* (2006) Imbalance between apoptosis and proliferation causes late radiation damage of salivary gland in mouse. Physiol Res **55**(1): 89–95.
27. Li J, *et al* (2005) Structural and functional characteristics of irradiation damage to parotid glands in the miniature pig. Int J Radiat Oncol Biol Phys **62**(5): 1510–1516.

Received on April 11, 2011
Revision received on October 4, 2011
Accepted on October 5, 2011

J Cancer Res Clin Oncol (2012) 138:1931–1936
DOI 10.1007/s00432-012-1277-0

ORIGINAL PAPER

Preliminary results of intensity-modulated radiation therapy with helical tomotherapy for prostate cancer

Natsuo Tomita · Norihito Soga · Yuji Ogura · Norio Hayashi · Hidetoshi Shimizu · Takashi Kubota · Junji Ito · Kimiko Hirata · Yukihiko Ohshima · Hiroyuki Tachibana · Takeshi Kodaira

Received: 5 May 2012 / Accepted: 21 June 2012 / Published online: 1 July 2012

Abstract
Purpose We present the preliminary results of intensity-modulated radiation therapy with helical tomotherapy (HT) for clinically localized prostate cancer.
Methods Regularly followed 241 consecutive patients, who were treated with HT between June 2006 and December 2010, were included in this retrospective study. Most patients received both relatively long-term neoadjuvant and adjuvant androgen deprivation therapy (ADT). Patients received 78 Gy in the intermediate high-risk group and 74 Gy in the low-risk group. Biochemical disease-free survival (bDFS) followed the Phoenix definition. Toxicity was scored according to the Radiation Therapy Oncology Group morbidity grading scale.
Results The median follow-up time from the start date of HT was 35 months. The rates of acute Grade 2 gastrointestinal (GI) and genitor-urinary (GU) toxicities were 11.2 and 24.5 %. No patients experienced acute Grade 3 or higher symptoms. The rates of late Grade 2 and 3 GI toxicities were 6.6 and 0.8 %, and those of late Grade 2 and 3 GU toxicities were 8.3 % and 1.2 %. No patients experienced late Grade 4 toxicity. The 3-year bDFS rates for low, intermediate, and high-risk group patients were 100, 100, and 95.8 %, respectively. We observed clinical relapse in two high-risk patients, resulting in a 3-year clinical DFS of 99.4 %.
Conclusions This preliminary report confirms the feasibility of HT in a large number of patients. We observed that HT is associated with low rates of acute and late toxicities, and HT in combination with relatively long-term ADT results in excellent short-term bDFS.

Keywords Prostate cancer · Intensity-modulated radiation therapy · Image-guided radiation therapy · Helical tomotherapy

N. Tomita (✉) · H. Shimizu · T. Kubota · J. Ito · K. Hirata · Y. Ohshima · H. Tachibana · T. Kodaira
Department of Radiation Oncology, Aichi Cancer Center Hospital, 1-1 Kanokoden, Chikusaku, Nagoya 464-8681, Japan
e-mail: ntomita@aichi-cc.jp

N. Soga · Y. Ogura · N. Hayashi
Department of Urology, Aichi Cancer Center Hospital, Nagoya, Japan

Introduction

High-dose external beam radiation therapy (EBRT) with intensity-modulated radiation therapy (IMRT) has been shown to improve disease-free survival in patients with localized prostate cancer over the past decade (Zelefsky et al. 2002; Alicikus et al. 2011). Helical tomotherapy (HT) is a novel IMRT treatment modality. HT is a form of 3D conformal radiation therapy in which treatment beams are spatially and temporally modulated to maximize the dose delivered to tumors while minimizing the dose delivered to normal structures (Kapatoes et al. 2001). In addition, detectors within the tomotherapy system provide megavoltage computed tomographic (MVCT) images of the patient, which can be obtained immediately before treatment for setup, registration, and repositioning [i.e., image-guided radiation therapy (IGRT)]. Thus, we believe that HT provides excellent target coverage with dose uniformity while sparing the organs at risk (OAR) and would avoid severe toxicity in patients with prostate cancer. On the other hand, IMRT has been used in Japan recently, especially for prostate cancer. However, to our knowledge, Japanese data of prostate cancer treated with IMRT have not been reported. In this report, we present the preliminary

results of IMRT with HT for clinically localized prostate cancer in Japan.

Materials and methods

Patients

Between June 2006 and December 2010, 251 patients with clinically localized prostate cancer were treated with HT at our institution. Of these, 10 patients were followed at their local hospital. Another 241 consecutive patients, who were followed regularly at our institution, were included in this retrospective study. Pretreatment diagnostic evaluations were performed by serum prostate-specific antigen (PSA), digital rectal examination, magnetic resonance imaging of the pelvis, computed tomography (CT) of the chest to the pelvis, and bone scintigraphy. All patients had histological diagnosis of prostatic adenocarcinoma, classified according to the Gleason grading system. The American Joint Committee on Cancer 2002 clinical staging was used, and patients were classified into three prognostic risk groups defined by the National Comprehensive Cancer Network criteria (http://www.nccn.org/) as follows: low, pretreatment PSA < 10 ng/ml, T1–T2a, and Gleason score ≤ 6; intermediate, T2b–T2c or Gleason score 7 or PSA 10–20 ng/ml; high, T3a or Gleason score 8–10 or PSA > 20 ng/ml. We classified patients with T3b–T4 clinical stage as a high-risk group in this study. Table 1 describes patient characteristics.

Table 1 Patient characteristics

Characteristic	$n = 241$
Age (years)	69 (49–81)
PSA level (ng/ml)	
<10	79 (32.8 %)
10–20	65 (27.0 %)
>20	97 (40.2 %)
Median	15.17
Range	1.40–502.00
Gleason score	
2–6	47 (19.5 %)
7	97 (40.2 %)
8–10	97 (40.2 %)
Tumor stage	
T1–T2a	73 (30.3 %)
T2b–T2c	36 (14.9 %)
T3a	97 (40.2 %)
T3b–T4	35 (14.6 %)
Risk group	
Low	17 (7.0 %)
Intermediate	53 (22.0 %)
High	171 (71.0 %)

Age data are presented as median values

Hormonal therapy

All patients were given neoadjuvant androgen deprivation therapy (N-ADT). A combination of a luteinizing hormone releasing hormone (LHRH) analogue and anti-androgen treatment (i.e., maximum androgen blockade) was performed as N-ADT. N-ADT time depended on the IMRT reservation in principle, and the median time of N-ADT was 9 months (range 2–68 months). Adjuvant ADT (A-ADT) consisted of only the LHRH analogue. Patients were given A-ADT for 1–2 years at the discretion of the urologists. Eight patients (3.3 %) did not receive A-ADT because they experienced adverse effects associated with N-ADT such as liver dysfunction, and 29 patients (12.0 %) continue to receive A-ADT at the time of this analysis. The median time of A-ADT in another patient was 20 months (range 1–37 months).

IMRT treatment

All patients were immobilized in a supine position with the Esform vacuum type immobilization system (Engineering System, Matsumoto, Japan) and simulated by pelvic computed tomography (CT) with a 2.5-mm slice thickness. On the day of CT simulation and during IMRT, all patients defecated where possible every morning and discharged urine about one hour before CT simulation and IMRT to minimize daily variations in the shape and anatomical location of the prostate. Outlines of the target were delineated on a 3-dimensional radiation treatment planning system (Pinnacle3 workstation, Hitachi Medical Corporation, Tokyo, Japan) using the abdominal CT window setting. Clinical target volume (CTV) was defined as the entire prostate and proximal seminal vesicle. In the case of seminal vesicle invasion, CTV included the entire seminal vesicle. Planning target volume 1 (PTV1) included CTV with a 6–8 mm margin except at the prostatorectal interface, where a 4–6 mm margin was used. PTV2 was defined as the seminal vesicle with a similar margin as PTV1 outside of PTV1. Normal structures including the rectum, bladder, femoral head, penile bulb, pubic bone, bowel, and sigmoid colon adjacent to PTV were considered to be OAR. The rectum was delineated only around PTV1 with 10 mm on the cranio-caudal direction. CT images and structure sets were transferred to the Tomotherapy Hi-Art System workstation (TomoTherapy Inc., Madison, WI, USA). Normal structures were constrained on an individual basis using maximum and dose–volume histogram (DVH) dose constraints without compromising PTV1 coverage.

The dose constraints required to achieve an acceptable HT plan in our institution were as follows: (1) PTV1 D95 (i.e., dose delivered to 95 % of PTV1): 74 Gy in the low-risk group, 78 Gy in intermediate and high-risk groups, maximum dose < 107 % of the prescribed dose, minimum dose > 90 % of the prescribed dose; (2) PTV2 D95: 64 Gy, minimum dose > 90 % of the prescribed dose; (3) rectum: the percentage of the entire rectum covered by at least 70 Gy (V70) < 15 %, V60 < 25 %, and V40 < 45 %; (4) bladder: the percentage of the entire bladder covered by at least 60 Gy (V60) < 25 % and V40 < 50 %; (5) femoral head: maximum dose < 40 Gy; (6) bowel, sigmoid colon: the volume covered by 55 Gy < 0.5 cc; (7) penile bulb: mean dose < 52.5 Gy; and (8) pubic bone: V70 < 20 %.

In tomotherapy treatment conditions, a 2.5-cm field width was used in all patients. Other common parameters were a pitch of 0.430 and a normal modulation factor of 2.0. The inverse planning system performed a variable number of iterations, which ranged from 100 to 300, during the optimization process for each plan. All patients began treatment with daily MVCT acquisitions for setup, registration, and repositioning on the basis of the location of the prostate. Patients inserted a tube or were encouraged to defecate when their rectums were dilated on MVCT and were checked on MVCT again.

Follow-up

Follow-up evaluations after treatment were performed at intervals of 3 months. Serum PSA was measured at each follow-up. The length of follow-up was calculated from the start date of IMRT. Biochemical disease-free survival (bDFS) followed the Phoenix definition (i.e., a post-treatment nadir plus 2.0 ng/ml Roach et al. 2006). A clinical relapse comprised local disease, and lymph node, bone, or parenchymal metastases detected by CT scan and/or bone scintigraphy. Patients began ADT again after documentation of biochemical relapse. Distributions of bDFS, disease-free survival (DFS), and overall survival were calculated according to the Kaplan–Meier method. The Student's t test was used in the analysis of prognostic factors for biochemical control. A p value of <0.05 was considered significant. Toxicity was scored according to the Radiation Therapy Oncology Group morbidity grading scale (Cox et al. 1995). In brief, Grade 1 toxicity represents minimal side effects not requiring medication for symptom control, Grade 2 toxicity indicates symptoms requiring medication, Grade 3 indicates complications requiring minor surgical intervention (i.e., transurethral resection, laser coagulation, or blood transfusion), and Grade 4 requires hospitalization and major intervention. The time to develop late toxicity was the interval from the start date of IMRT.

Results

The prescribed dose was slightly reduced to 74 or 70 Gy in 16 patients (6.6 %) because of their antithrombogenic medications (6 patients), failure in OAR dose constraints (4 patients, especially in those whose bowel or sigmoid colon invaginated into the surrounding area of PTV1), patients' request or physicians' suggestion for their acute rectal symptoms (3 patients), financial reasons (one patient), and unspecified in 2 patients. The median IMRT period was 57 days (range 51–95 days). The median follow-up time from the start date of IMRT was 35 months (range 13–66 months).

Acute toxicity

Table 2 shows the incidence of acute gastro-intestinal (GI) and genitor-urinary (GU) toxicities treated with IMRT with HT. Of 27 patients (11.2 %) who developed acute Grade 2 rectal toxicity requiring medication such as suppositories, the main symptoms were pain on defecation in 17 patients (7.1 %) and rectal bleeding with bowel movements in 10 patients (4.1 %), respectively. Of 59 patients (24.5 %) who developed acute Grade 2 urinary toxicity, most symptoms (55, 22.7 %) were dysuria such as urinary frequency, and other symptoms were gross hematuria in 3 patients (1.2 %) and pain with urination in 2 patients (0.8 %). No patients experienced acute Grade 3 or higher acute symptoms.

Late toxicity

The incidence of late GI and GU toxicities is also shown in Table 2. Of 16 patients (6.6 %) who developed late Grade 2 rectal toxicity, 13 patients (5.4 %) developed Grade 2 rectal bleeding at a median of 18 months (range 10–39 months) after the start date of IMRT. Other symptoms were pain on defecation in 2 patients (0.8 %) after 9 and 11 months and subtle fecal incontinence in one patient (0.4 %) after 9 months. Two patients (0.8 %) developed Grade 3 rectal bleeding requiring laser coagulation at 11

Table 2 Incidence of acute and late Grade 2 or higher gastro-intestinal (GI) and genitor-urinary (GU) toxicity among patients treated with intensity-modulated radiation therapy (IMRT) with helical tomotherapy ($n = 241$)

	Acute toxicity		Late toxicity	
	GI	GU	GI	GU
Grade 2	27 (11.2 %)	59 (24.5 %)	16 (6.6 %)	20 (8.3 %)
Grade 3	0 (0 %)	0 (0 %)	2 (0.8 %)	3 (1.2 %)
Grade 4	0 (0 %)	0 (0 %)	0 (0 %)	0 (0 %)
Total	27 (11.2 %)	59 (24.5 %)	18 (7.4 %)	23 (9.5 %)

Table 3 Patient characteristics with or without biochemical relapse after intensity-modulated radiation therapy (IMRT) with helical tomotherapy

Characteristic	Biochemical relapse group ($n = 6$)	Biochemical control group ($n = 169$)	p value
Age (years)	65 (51–77)	69 (49–81)	0.041
PSA level (ng/ml)	38.26 (24.88–153.00)	15.17 (1.40–502.00)	0.057
Gleason score	9 (8–10)	7 (5–10)	0.0030
Tumor stage			0.00022
T1–T2c	0 (0 %)	82 (50.3 %)	
T3a	2 (33.3 %)	63 (38.7 %)	
T3b–T4	4 (66.7 %)	18 (11.0 %)	
Risk group			0.13
Low	0 (0 %)	14 (8.2 %)	
Intermediate	0 (0 %)	39 (23.0 %)	
High	6 (100 %)	113 (68.8 %)	

and 12 months after the start date of IMRT. No Grade 4 late rectal complications have been observed. Of 20 patients (8.3 %) who developed late Grade 2 urinary toxicity, 16 patients (6.6 %) experienced dysuria requiring medication at a median of 19 months (range 7–47 months) after the start date of IMRT. Other symptoms were gross hematuria in 2 patients (0.8 %) and cystitis in 2 patients (0.8 %). Two patients (0.8 %) experienced Grade 3 urinary retention requiring self-catheterization or dilation at 14 and 17 months after the start date of IMRT. One patient developed a bladder ulcer (Grade 3) requiring laser coagulation after 14 months. No patients experienced late Grade 4 urinary symptoms.

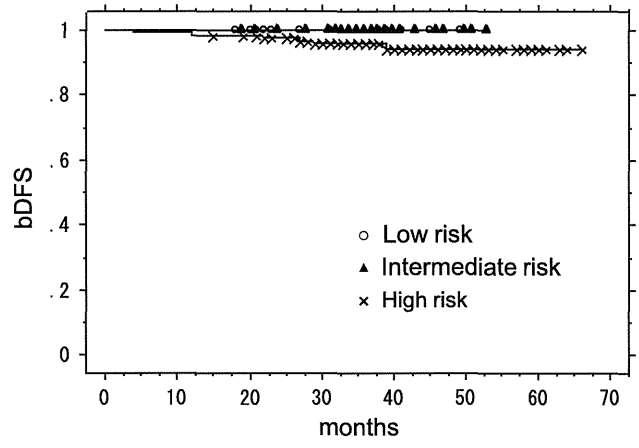

Fig. 1 The 3-year biochemical disease-free survival (bDFS) for low, intermediate, and high-risk group patients

Biochemical control, clinical relapse, and overall survival

Biochemical control was estimated in only 175 patients followed for at least 6 months after the completion of A-ADT. Six patients in the high-risk group developed biochemical relapse at a median of 25 months (range 4–39) after the start date of IMRT. No patients in low and intermediate risk groups experienced biochemical relapse. Table 3 shows each patient's characteristics with or without biochemical relapse. Age, Gleason score, and T-stage were significant factors of biochemical relapse in patient characteristics ($p = 0.041$, 0.0030, and 0.00022, respectively). PSA in the biochemical relapse group seemed to be higher than those in the biochemical control group, but PSA and the risk group had no significant impact on the biochemical control.

The 3-year bDFS rate was 96.9 % (95 % confidence interval (CI): 94.2–99.6 %) in all groups. The 3-year bDFS rates for low, intermediate, and high-risk group patients were 100, 100, and 95.8 % (CI: 92.1–99.5 %), respectively. The bDFS for each risk group are shown in Fig. 1. We observed clinical relapse in two patients in the high-risk group, resulting in a 3-year clinical DFS of 99.4 % (CI: 98.2–100 %). One patient developed bone metastasis of the humerus after 4 months, and the other patient developed pelvic node metastases after 39 months. Each patient received ADT after clinical relapse. No patient died at the time of analysis, resulting in a 3-year OS of 100 %.

Discussion

We could not find a published report for Japanese outcomes of prostate cancer treated with IMRT in a PubMed search, although there were many reports of permanent brachytherapy. Therefore, to our knowledge, this data may be the first report to compile IMRT-treated patients in Japan and demonstrate the feasibility of high-dose radiotherapy with HT for patients with localized prostate cancer. Localized prostate cancer patients, especially those in the low-risk group, usually have some radical treatment choices such as radical prostatectomy, IMRT, brachytherapy, particle therapy, and recently implemented robotic surgery. This report provided outcomes and toxicities for localized

prostate cancer after IMRT with IGRT (i.e., HT) combined with ADT in one of the Japanese cancer centers, and this could be the basis of comparison with other treatments and will be of assistance for patients and physicians associated with prostate cancer at the time for treatment choice.

Most patients could receive the prescribed total doses, but they were slightly reduced in 16 patients (6.6 %). To our knowledge, the impact of antithrombogenic medication on GI toxicity is still uncertain. The total doses of some patients who took this medication were reduced based on each physician's clinical decision. We will estimate the impact of the antithrombogenic medication on toxicity circumstantially in the near future. Some patients received a reduced total dose because of their acute rectal symptoms. Zelefsky et al. (2008) recently reported that the presence of acute GI and GU symptoms during treatment conferred a fivefold and threefold increased risk of late GI and GU toxicities, respectively, in 1,571 patients with prostate cancer who had a long follow-up after receiving 3-dimensional conformal radiotherapy (3DCRT) or IMRT. Therefore, we think that these patients would have developed severe late GI toxicity if they had received the prescribed total dose. We will also estimate the relationship between acute and late toxicity for patients treated with HT. We reduced the total dose for some patients due to failure in OAR dose constraints, especially in patients whose bowel or sigmoid colon invaginated into the surrounding area of PTV1. We think that these patients should choose other treatments such as surgery if possible.

We observed a satisfactory low rate in acute GI and GU toxicity, and the Grade 2 rates of acute GI and GU toxicity were 11.2 and 24.5 %, respectively. Among patients who developed acute Grade 2 rectal toxicity, the main symptoms were pain on defecation. We think from our clinical experience that these symptoms were not so much due to the doses exposed to the rectum, but rather too much effort from each patient's to empty their bowels because they had inserted a tube or were encouraged to defecate when their rectums were dilated on MVCT. On the other hand, we observed a satisfactory low rate in late GI and GU toxicity, and the rates of late Grade 2 or higher GI and GU toxicity were only 7.4 and 9.5 %, respectively. Data indicate that late rectal toxicity profiles are excellent compared to the incidence of late Grade 2 or higher GU and GI toxicity that reportedly ranged from 24 to 35 % and from 15 to 29 %, respectively, in recent studies with the use of IMRT (Vora et al. 2007; Wong et al. 2009; Sharma et al. 2011). We think that our favorable toxicity rates came partly as a result of IGRT with HT. The significance of IGRT is established in EBRT for localized prostate cancer (http://www.nccn.org/). However, IGRT was conducted at only approximately 60 % of facilities in a recent Japanese national survey on the current status of EBRT for prostate cancer (Nakamura et al. 2012). Another may be the relatively tight margin used between CTV and PTV. Enmark et al. (2006) demonstrated that a margin of 4 mm in all directions was adequate to account for uncertainties including inter- and intra-fraction motions. In a recent report (Crehange et al. 2012), 165 men were treated with daily IMRT with IGRT using a 3D ultrasound-based system and stratified regarding CTV to PTV margin: group A, 5 mm or group B, 10 mm. Their data indicated that the margin had no impact on short-term bDFS in control of IGRT. We also confirmed favorable short-term bDFS in the current report. However, long-term follow-up is required to evaluate the clinical significance of the tight margin with IGRT.

Our preliminary results suggest excellent short-term biochemical out-comes for all risk group patients when treated with HT combined with relatively long-term ADT. Of course, longer follow-up will be necessary to determine whether HT results in an incremental favorable outcome in tumor control. Actually, in our clinical experience of 3DCRT (Tomita et al. 2009), patients develop biochemical relapse 4–5 years after the start date of RT when combined with long-term (>2 years) ADT. All patients who developed biochemical relapse were in the high-risk group in this cohort, and age, Gleason score, and T-stage were significant factors of biochemical relapse in patient characteristics. Ogawa et al. (2011) surveyed the pattern of care study (PCS) for radical EBRT for clinically localized prostate cancer in Japan. They reported that the number of patients in the high-risk group consisted of more than 60 % of the 2003–2005 survey, although the number of patients in the high-risk group decreased gradually. The current study cohort was similar to that of PCS. There is room for consideration of the treatment strategy for high-risk prostate cancer patients in Japan.

In conclusion, this preliminary report confirms the feasibility of HT in a large number of localized prostate cancer patients. We observed that HT is associated with low rates of acute and late toxicities, and HT in combination with relatively long-term ADT results in excellent short-term bDFS. Superior dose distributions and IGRT with HT are better options not only for high-dose EBRT, but also for all treatment choices of localized prostate cancer.

Conflict of interest We declare that we have no conflict of interest.

References

Alicikus ZA, Yamada Y, Zhang Z, Pei X, Hunt M, Kollmeier M, Cox B, Zelefsky MJ (2011) Ten-year outcomes of high-dose, intensity-modulated radiotherapy for localized prostate cancer. Cancer 117(7):1429–1437

Cox JD, Stetz J, Pajak TF (1995) Toxicity criteria of the Radiation Therapy Oncology Group (RTOG) and the European Organization for Research and Treatment of Cancer (EORTC). Int J Radiat Oncol Biol Phys 31(5):1341–1346

Crehange G, Mirjolet C, Gauthier M, Martin E, Truc G, Peignaux-Casasnovas K, Azelie C, Bonnetain F, Naudy S, Maingon P (2012) Clinical impact of margin reduction on late toxicity and short-term biochemical control for patients treated with daily online image guided IMRT for prostate cancer. Radiother Oncol 103(2):244–246

Enmark M, Korreman S, Nystrom H (2006) IGRT of prostate cancer; is the margin reduction gained from daily IG time-dependent? Acta Oncol 45(7):907–914

Kapatoes JM, Olivera GH, Ruchala KJ, Smilowitz JB, Reckwerdt PJ, Mackie TR (2001) A feasible method for clinical delivery verification and dose reconstruction in tomotherapy. Med Phys 28(4):528–542

Nakamura K, Akimoto T, Mizowaki T, Hatano K, Kodaira T, Nakamura N, Kozuka T, Shikama N, Kagami Y (2012) Patterns of practice in intensity-modulated radiation therapy and image-guided radiation therapy for prostate cancer in Japan. Jpn J Clin Oncol 42(1):53–57

National Comprehensive Cancer Network. NCCN clinical practice guidelines in oncology: prostate cancer V1 2011. http://www.nccn.org/. Accessed 10 April 2012

Ogawa K, Nakamura K, Sasaki T, Onishi H, Koizumi M, Araya M, Mukumoto N, Teshima T, Mitsumori M (2011) Radical external beam radiotherapy for clinically localized prostate cancer in Japan: changing trends in the patterns of care process survey. Int J Radiat Oncol Biol Phys 81(5):1310–1318

Roach M 3rd, Hanks G, Thames H Jr, Schellhammer P, Shipley WU, Sokol GH, Sandler H (2006) Defining biochemical failure following radiotherapy with or without hormonal therapy in men with clinically localized prostate cancer: recommendations of the RTOG–ASTRO phoenix consensus conference. Int J Radiat Oncol Biol Phys 65(4):965–974

Sharma NK, Li T, Chen DY, Pollack A, Horwitz EM, Buyyounouski MK (2011) Intensity-modulated radiotherapy reduces gastrointestinal toxicity in patients treated with androgen deprivation therapy for prostate cancer. Int J Radiat Oncol Biol Phys 80(2):437–444

Tomita N, Kodaira T, Tachibana H, Nakamura T, Tomoda T, Nakahara R, Inokuchi H, Hayashi N, Fuwa N (2009) Dynamic conformal arc radiotherapy with rectum hollow-out technique for localized prostate cancer. Radiother Oncol 90(3):346–352

Vora SA, Wong WW, Schild SE, Ezzell GA, Halyard MY (2007) Analysis of biochemical control and prognostic factors in patients treated with either low-dose three-dimensional conformal radiation therapy or high-dose intensity-modulated radiotherapy for localized prostate cancer. Int J Radiat Oncol Biol Phys 68(4):1053–1058

Wong WW, Vora SA, Schild SE, Ezzell GA, Andrews PE, Ferrigni RG, Swanson SK (2009) Radiation dose escalation for localized prostate cancer: intensity-modulated radiotherapy versus permanent transperineal brachytherapy. Cancer 115(23):5596–5606

Zelefsky MJ, Fuks Z, Hunt M, Yamada Y, Marion C, Ling CC, Amols H, Venkatraman ES, Leibel SA (2002) High-dose intensity modulated radiation therapy for prostate cancer: early toxicity and biochemical outcome in 772 patients. Int J Radiat Oncol Biol Phys 53(5):1111–1116

Zelefsky MJ, Levin EJ, Hunt M, Yamada Y, Shippy AM, Jackson A, Amols HI (2008) Incidence of late rectal and urinary toxicities after three-dimensional conformal radiotherapy and intensity-modulated radiotherapy for localized prostate cancer. Int J Radiat Oncol Biol Phys 70(4):1124–1129